

Dual-energy X-ray absorptiometry prediction of adipose tissue depots in children and adolescents

Jacqueline Bauer¹, John Thornton¹, Steven Heymsfield², Kim Kelly¹, Alexander Ramirez¹, Sonia Gidwani¹ and Dympna Gallagher¹

BACKGROUND: The measurement of adipose tissue (AT) depots *in vivo* requires expensive imaging methods not accessible to most clinicians and researchers. The study aim was to derive mathematical models to predict total AT (TAT) and subdepots from total body fat derived from a dual-energy X-ray absorptiometry (DXA) scan.

METHODS: Models were developed to predict magnetic resonance imaging–derived TAT and subdepots subcutaneous AT, visceral AT, and intermuscular AT from DXA total body fat (Fat_{DXA}) using cross-sectional data (time 0 (T0)) and validated results using 1 (T1) and 2 (T2) y follow-up data. Subjects were 176 multiethnic healthy children ages 5–17 y at T0. Twenty-two were measured at T1 and T2. TAT was compared with Fat_{DXA} .

RESULTS: At T0, TAT was greater than Fat_{DXA} (12.5 ± 8.4 vs. 12.0 ± 9.4 kg; $P < 0.0001$), with a quadratic relationship between TAT and Fat_{DXA} that varied by sex. Predicted mean TATs were not different from measured TATs: T1: (9.84 ± 4.45 kg vs. 9.50 ± 4.37 kg; $P = 0.11$); T2: (12.94 ± 6.75 kg vs. 12.89 ± 7.09 kg; $P = 0.76$). The quadratic relationship was not influenced by race or age.

CONCLUSION: In general, the prediction equations for TAT and subdepots were consistent with the measured values using T1 and T2 data.

Childhood obesity continues to increase at an alarming rate, having reached epidemic levels in many countries, and it demands attention worldwide (1). Excess weight gain during childhood is one of the most serious global health problems. There is growing evidence that body fat or adipose tissue (AT) accumulation, especially visceral or intra-abdominal AT accumulation, correlates with overweight and obesity, and is an indirect marker of metabolic diseases in adulthood. Both the total amount of AT and its distribution are risk factors for several metabolic disturbances. Excess accumulation of lipids in visceral AT is related to impaired insulin sensitivity (a precursor to the development of type 2 diabetes) and unfavorable lipid metabolism in children (2–4). Intermuscular AT (IMAT) is negatively associated with insulin sensitivity in black adolescents (5).

Accordingly, appropriate and accurate techniques to determine body composition in infants and adolescents are needed

for a greater comprehension of the mechanisms by which key conditions in infancy regulate and mediate AT distribution, the characterization of the severity of adiposity or malnutrition, and the evaluation of the efficacy of interventional strategies in the pediatric population. Nutritional status in children can be evaluated by means of simple anthropometric assessment methods. BMI, an index of excess weight relative to height, has a moderately high sensitivity for the general identification of the obese child, but a weak correlation with total body fat due to considerable changes in fat mass that occur during childhood (6). Body weight and BMI are insufficiently sensitive markers for the evaluation of fat distribution in children, as both are influenced by changes in body cell mass during growth (7). Waist circumference is used as a surrogate for abdominal fat mass in adults where the latter is associated with elevated risk for cardiovascular disease and abnormalities of glucose and lipids metabolism (8,9). However, the more potent visceral AT may differ in quantity among individuals with similar waist circumference (10).

As compared with adults, children have greater variations in body composition (including fat and lean tissues) due to maturation, growth, puberty, and gender, which decrease the accuracy for the estimation of total or abdominal fat using anthropometric assessment methods (11,12). Reliable assessments for quantification of fat distribution during childhood include computerized tomography and magnetic resonance imaging (MRI). Unfortunately, MRI is expensive and requires sedation in young infants; with computerized tomography, a relatively high radiation exposure is required that prohibits its use in pediatric studies (13). In several clinical and research trials, dual-energy X-ray absorptiometry (DXA) has been used for the estimation of total and regional body composition in children with a relatively rapid scan time, minimal radiation exposure, and good reproducibility (14–16). Nevertheless, DXA does not allow for the separation of subcutaneous AT (SAT) from visceral AT (VAT).

Therefore, the need for an accurate, safe, and a cost-effective approach for the assessment of AT distribution exists. During obesity treatment programs in children and adolescents, there is increasing interest in monitoring changes in body composition.

¹New York Obesity Nutrition Research Center, St. Luke's-Roosevelt Hospital, Columbia University, New York, New York; ²Pennington Biomedical Research Center, Baton Rouge, Louisiana. Correspondence: Dympna Gallagher (dg108@columbia.edu)

As DXA is the most commonly used body composition measurement method, the proposed AT distribution models could be useful in research and clinical settings where the need exists to estimate the size of the VAT or IMAT depots with respect to metabolic risk assessment in children and adolescents.

The aim of our investigation in this pediatric cohort was to derive models to predict MRI-derived total AT and subdepots (SAT, VAT, and IMAT) from DXA total body fat using cross-sectional data and to validate findings by means of longitudinal data.

RESULTS

Subject Characteristics

Percentile of BMI was calculated for each child during the investigation period.

Cross-sectional. The baseline (time 0 (T0)) study group included 176 healthy children and young adults ages 5–17 y. Characteristics of the participant are presented in **Table 1**. At baseline, Tanner classification was available on 77% ($n = 135$) of participants; 47% of the children were at stage 1, 10% at stage 2, 9% at stage 3, 8% at stage 4, and 26% at stage 5.

Longitudinal. Twenty-nine participants with T0 data were measured longitudinally; 15 with measures at T0, T2, and T2; 7 with measures at T0 and T1, and 7 with measures at T0 and T2. At T1, 73% of the 22 children were at Tanner stage 1, and at T2, 60% of the 20 children with Tanner stage data were at stage 1.

Separate analyses were conducted on the total cohort and on the subgroup where Tanner stage was available. Tanner stage as an independent variable in the models did not contribute

significantly to the prediction equations for the subgroup; therefore, the prediction equations based on the total group are presented.

Adipose Tissue and Fat

Mean values for total AT (TAT), subdepots (SAT, VAT, and IMAT) and for Fat_{DXA} (total body fat from DXA) are presented in **Table 2**. At baseline, TAT was greater than Fat_{DXA} (12.5 ± 8.4 vs. 12.0 ± 9.4 kg; $P < 0.0001$), with a quadratic relationship between TAT and fat ($\text{TAT} = a_0 + a_1 \times \text{fat} + a_2 \times \text{fat}^2$; $r^2_{\text{PRESS}} = 0.99$, $\text{SEE}_{\text{PRESS}} = 1.01$ kg), where PRESS is the predicted residual sum of squares and $\text{SEE}_{\text{PRESS}}$ is the standard error of the estimate for PRESS. The relationship varied by sex (**Figure 1**): equation coefficients (a_0 , a_1 , and a_2) for females are (2.191, 0.776, and 0.003) and for males are (2.641, 0.792, and 0.002) as presented in **Table 3**. Predicted mean TATs were not different from measured TATs: T1: (9.84 ± 4.45 kg vs. 9.50 ± 4.37 kg; $P = 0.11$). Descriptive statistics for the difference, predicted minus measured, are mean (0.34 kg), SD (0.97 kg), and interquartile range (1.28 kg). T2: (12.94 ± 6.75 kg vs. 12.89 ± 7.09 kg; $P = 0.76$). Descriptive statistics for the difference, predicted minus measured, are mean (0.06 kg), SD (0.83 kg), and interquartile range (0.93 kg). The quadratic relationship was not influenced by race or age.

DXA Prediction of Adipose Tissue Subdepots

The prediction equations for the subdepots are presented in **Table 3**. Age was a significant predictor in the SAT quadratic model. Both VAT and IMAT equations were derived using the natural logarithm of the dependent variable. Race was a significant predictor of $\text{Log}(\text{VAT})$. Neither age nor race were

Table 1. Characteristics of the subjects by gender

| Characteristic | Follow-up points | | | | | |
|--------------------------|--------------------|--------------------|-------------------|-------------------|--------------------|-------------------|
| | Baseline (T0) | | 1 y (T1) | | 2 y (T2) | |
| | Girls ($n = 73$) | Boys ($n = 103$) | Girls ($n = 8$) | Boys ($n = 14$) | Girls ($n = 5$) | Boys ($n = 17$) |
| Age (y) (range) | 10.6 ± 3.3 (6–17) | 11.2 ± 3.4 (5–17) | 8.6 ± 1.2 (7–11) | 9.4 ± 1.4 (7–11) | 11.0 ± 1.0 (10–12) | 10.6 ± 1.2 (9–12) |
| Weight (kg) | 43.6 ± 18.7 | 47.6 ± 20.2 | 35.7 ± 11.4 | 34.2 ± 7.9 | 44.8 ± 14.2 | 43.0 ± 12.3 |
| Height (cm) | 127.8 ± 9.1 | 129.1 ± 11.1 | 137.9 ± 9.7 | 137.2 ± 8.9 | 147.9 ± 11.7 | 144.8 ± 10.1 |
| BMI percentile | 64.5 ± 28.5 | 63.1 ± 28.4 | 56.4 ± 34.7 | 61.6 ± 23.5 | 72.9 ± 30.2 | 66.5 ± 29.7 |
| Tanner stage ($n, \%$) | | | | | | |
| 1 | 29, 46.0 | 35, 48.6 | 5, 62.5 | 11, 78.6 | 2, 50.0 | 10, 62.5 |
| 2 | 6, 9.5 | 8, 11.1 | 2, 25.0 | 2, 14.3 | 1, 25.0 | 2, 12.5 |
| 3 | 5, 7.9 | 8, 11.1 | 1, 12.5 | 1, 7.1 | 1, 25.0 | 4, 25.0 |
| 4 | 5, 7.9 | 6, 8.3 | 0, 0 | 0, 0 | 0, 0 | 0, 0 |
| 5 | 18, 28.6 | 15, 20.8 | 0, 0 | 0, 0 | 0, 0 | 0, 0 |
| Ethnicity (n) | | | | | | |
| Caucasian | 9 | 17 | 1 | 2 | 0 | 2 |
| Black | 32 | 37 | 3 | 2 | 1 | 2 |
| Hispanic | 20 | 32 | 1 | 8 | 1 | 10 |
| Asian | 6 | 7 | 2 | 2 | 3 | 2 |
| Other | 6 | 10 | 1 | 0 | 0 | 0 |

Table 2. Adipose tissue and subdepots by MRI and fat by DXA

| | Follow-up points | | | | | |
|-------------------------|------------------|----------------|---------------|---------------|---------------|---------------|
| | Baseline (T0) | | 1 y (T1) | | 2 y (T2) | |
| | Girls (n = 73) | Boys (n = 103) | Girls (n = 8) | Boys (n = 14) | Girls (n = 5) | Boys (n = 17) |
| Fat _{DXA} (kg) | 13.7 ± 10.2 | 10.8 ± 8.6 | 10.1 ± 6.0 | 8.4 ± 5.0 | 17.0 ± 8.6 | 11.2 ± 7.4 |
| TAT (kg) | 13.8 ± 9.3 | 11.5 ± 7.5 | 10.3 ± 4.5 | 9.0 ± 4.4 | 16.7 ± 7.9 | 11.8 ± 6.7 |
| SAT (kg) | 12.8 ± 8.7 | 10.5 ± 6.7 | 9.7 ± 4.3 | 8.2 ± 3.9 | 15.5 ± 7.5 | 10.8 ± 6.0 |
| VAT (kg) | 0.46 ± 0.39 | 0.51 ± 0.42 | 0.35 ± 0.19 | 0.47 ± 0.34 | 0.64 ± 0.50 | 0.59 ± 0.56 |
| IMAT (kg) | 0.51 ± 0.45 | 0.48 ± 0.42 | 0.28 ± 0.16 | 0.30 ± 0.17 | 0.47 ± 0.22 | 0.37 ± 0.24 |

Results are given as mean ± SD.

DXA, dual-energy X-ray absorptiometry; Fat_{DXA}, total body fat from DXA; IMAT, intermuscular adipose tissue; MRI, magnetic resonance imaging; SAT, subcutaneous adipose tissue; TAT, MRI total adipose tissue; VAT, visceral adipose tissue.

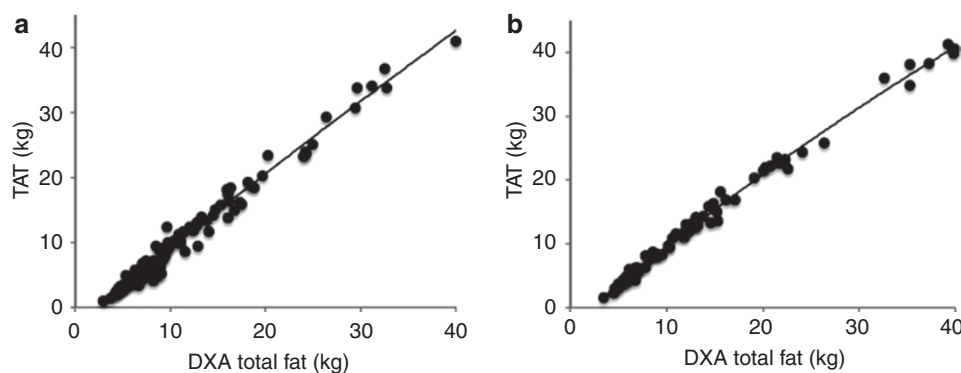


Figure 1. Relations (quadratic) between fat by dual-energy X-ray absorptiometry (DXA) and total adipose tissue (TAT) by magnetic resonance imaging in (a) males and (b) females. (a) Males: $TAT (kg) = 2.64 + 0.79 \times fat (kg) + 0.002 \times fat (kg)^2$ ($R^2_{PRESS} = 0.99$, $P < 0.0001$; $SEE_{PRESS} = 1.01$ kg, $n = 103$). (b) Females: $TAT (kg) = 2.19 + 0.78 \times fat (kg) + 0.003 \times fat (kg)^2$ ($R^2_{PRESS} = 0.99$, $P < 0.0001$; $SEE_{PRESS} = 1.01$ kg, $n = 73$). PRESS, predicted residual sum of squares; SEE_{PRESS} , standard error of the estimate for PRESS.

significant predictors of Log(IMAT). The r^2_{PRESS} for the prediction equations for subdepots were SAT (0.99), VAT (0.72), and IMAT (0.75).

SAT. A comparison of predicted SAT to measured SAT by sex revealed no significant differences at 1-y ($P = 0.2173$) and at 2-y ($P = 0.7793$) follow-up.

VAT. No significant differences were found for the comparison of predicted Log(VAT) and measured Log(VAT) by sex at 1-y ($P = 0.7604$) or 2-y ($P = 0.2134$) follow-up.

IMAT. At 1-y follow-up, there was a significant difference between predicted and measured Log(IMAT) for females ($P = 0.0170$). Although there was no significant difference between predicted and measured Log(IMAT) for males, there was a statistical trend suggesting a difference ($P = 0.06026$). In contrast, at 2-y follow-up there was a significant difference between predicted and measured Log(IMAT) for males ($P = 0.0184$). There was a statistical trend suggesting a difference for females ($P = 0.0816$).

DISCUSSION

This study provides for the first time useful prediction equations for estimating total AT and its subdepots in a pediatric

population. These data indicate that DXA fat values can be applied to obtain estimates for MRI-derived AT mass in healthy children and adolescents during development.

Prediction of Adipose Tissue in 5–17-Year-Old Children and Adolescents

A principal finding of this study is that predicted TAT does not differ from measured TAT, with a quadratic relationship found between TAT and Fat_{DXA}. That is, TAT can be predicted from Fat_{DXA} and this relationship varies by sex. For a given amount of Fat_{DXA}, males will have a higher predicted TAT than females. Our findings suggest that the association between TAT and Fat_{DXA} does not change with development, and no significant differences were detected by race.

At baseline and follow-up time points, TAT measures by MRI were on average 4% greater than fat values measured by DXA, exhibiting generally higher values for girls than for boys with both techniques. These sex differences are in agreement with previous reports during childhood (17,18). Comparisons of whole DXA fat and MRI-measured TAT in adults have been reported in the literature indicating that DXA and MRI AT values are highly correlated (19–21). In a study of adult HIV-infected patients and healthy controls, DXA-estimated peripheral fat was consistently larger than MRI-estimated AT in regional body fat depots. Moreover, with increasing levels

Table 3. Prediction models for MRI-derived adipose tissue depots

| Models and variables | a0 | a1 | a2 | a3 | r^2_{PRESS} | SEE _{PRESS} |
|--|-------|------|---------|------|---------------|----------------------|
| TAT = a0 + a1 × fat + a2 × fat ² | | | | | 0.99 | 1.01 |
| Females | 2.19 | 0.78 | 0.003 | | | |
| Males | 2.64 | 0.79 | 0.002 | | | |
| SAT = a0 + a1 × fat + a2 × fat ² + a3 × age | | | | | 0.99 | 0.90 |
| Females | 1.88 | 0.67 | 0.0043 | 0.05 | | |
| Males | 1.98 | 0.72 | 0.0013 | 0.05 | | |
| Log (VAT) = a0 + a1 × fat + a2 × fat ² | | | | | 0.72 | 0.44 |
| African American | | | | | | |
| Females | −2.76 | 0.17 | −0.0028 | | | |
| Males | −2.52 | 0.17 | −0.0028 | | | |
| Asian, Caucasian | | | | | | |
| Females | −2.26 | 0.17 | −0.0028 | | | |
| Males | −2.02 | 0.17 | −0.0028 | | | |
| Hispanic | | | | | | |
| Females | −2.60 | 0.17 | −0.0028 | | | |
| Males | −2.36 | 0.17 | −0.0028 | | | |
| Other | | | | | | |
| Females | −2.26 | 0.17 | −0.0028 | | | |
| Males | −2.02 | 0.17 | −0.0028 | | | |
| Log (IMAT) = a0 + a1 × fat + a2 × fat ² | | | | | 0.75 | 0.38 |
| Females | −2.21 | 0.12 | −0.0013 | | | |
| Males | −2.05 | 0.12 | −0.0013 | | | |

a0 is the constant term, a1 is the coefficient of fat (by dual-energy X-ray absorptiometry), a2 is the coefficient of fat², and a3 is the coefficient of age in the prediction equations. Log (x) indicates the natural logarithm of x.

IMAT, intermuscular adipose tissue; MRI, magnetic resonance imaging; PRESS, predicted residual sum of squares; SAT, subcutaneous adipose tissue; SEE_{PRESS}, standard error estimate for PRESS; TAT, total adipose tissue; VAT, visceral adipose tissue.

of fat mass, the differences between DXA fat and MRI-derived AT were greater (22). Postulated mechanisms include inability of MRI to detect small AT depots (e.g., intramuscular or liver fat depots) below the resolution of MRI; therefore, these fat amounts are not included in MRI estimates (22). DXA has been found to underestimate fat mass in leaner children and overestimate fat mass in heavier subjects (23).

We show that fat mass measured by DXA is useful for predicting, not exclusively TAT but also the subdepots SAT, VAT, and IMAT, where VAT and IMAT were modeled using the natural logarithm. The prediction of AT subdepots revealed that SAT varied by age and sex, and VAT varied by sex and race. Race influenced only VAT values, with Africans Americans having less VAT than Hispanics, Caucasians, Asians, and Others, when fat is held constant. The one exception was IMAT, as the equation in this case did not predict values that agreed with the measured data at follow-up.

Prediction of AT With Longitudinal Evaluation

In a small sample of predominantly prepubertal children followed over 2 y, predicted mean TAT values were consistent with the measured TAT values at each time point. The results were not influenced by race or sex. Therefore, the predicted

TAT for a given amount of total body fat was equivalent for males and females of differing races; however, males have more TAT than females for the same amount of total body fat. VAT and IMAT were not influenced by age. In general, the AT sub-depot prediction equations were valid using longitudinal data. However, we acknowledge that the sample size was small, with few children in some age groups and developmental stages.

Strengths and Limitations

DXA offers some advantages over MRI as a means of estimating fat distribution, including easier access to an instrument, an uncomplicated test technique for children as no cooperation is required, and a relatively low cost. A limitation of DXA is, however, the radiation exposure to the child, which despite being low ($\leq 15 \mu\text{Sv}$ per whole-body scan for a child as compared with $20 \mu\text{Sv}$ for a chest X-ray), is unattractive for some parents (24). The technique is attractive and valuable for providing measurements of longitudinal changes in body composition, both at the total body and regional level (22,25). Our study used the longitudinal measurements that were available on a subset of the sample rather than an independent sample in a validation study, which we acknowledge as a limitation.

Conclusion

Fat mass measured by DXA is useful for predicting TAT, SAT, and VAT. For the pediatric population it is possible to translate the fat measurement into predicted TAT, SAT, and VAT values that are expected to agree with measured TAT, SAT, and VAT, but this is not so for IMAT. For longitudinal studies in the pediatric population, DXA is an advantageous technique for the assessment of body compositional changes that occur during childhood.

METHODS

Protocol

Subjects included in this analysis participated in one of two studies in which the protocols involved the same whole-body MRI protocol and whole-body DXA scan. Study 1 was a cross-sectional study (baseline data only, T0) and Study 2 employed a longitudinal design and participants were evaluated at baseline (T0), 1-y (T1) and 2-y (T2). The T0 data presented in this analysis represent combined data from both studies. The T1 and T2 data are from Study 2 only.

All medical and body composition evaluations were carried out on the same day with the subject clothed in a hospital gown and without shoes. Subjects reported for testing to the Body Composition Unit, St. Luke's-Roosevelt Hospital Center. The studies were approved by the Institutional Review Board of St. Luke's-Roosevelt Hospital (IRB no. 00-069 and IRB no. 03-072). Verbal assent was obtained from all participating children and young adults before participation, and their parents provided written consent.

Subjects

Subjects were a multiethnic group of 176 healthy children and young adults ($n = 137$ from Study 1 and $n = 39$ from Study 2). All participants were recruited through schools, local area newspaper advertisements, and flyers dispersed in different locations in the local community. Subjects were required to be ambulatory, free of medical conditions or metabolic disorders (e.g., acute or chronic diseases), and not taking medications that could potentially affect the variables under investigation.

At each study point, body weight was measured using a scale (Avery Weight-Tronix digital scale, model DS-01, Pointe-Claire, Quebec, Canada) to the nearest 0.1 kg, and height was measured using a wall-mounted stadiometer (235 Heightronic Digital Stadiometer, Quick Medical and Measurement Concepts, Snoqualmie, WA) to the nearest 0.1 cm. Pubertal status was evaluated by a pediatrician using the Tanner criteria at baseline and at follow-up points. Ethnicity was assessed by questionnaire reporting of the ethnic background of the child.

DXA

Total body fat content was estimated in all children with a whole-body scanner (Lunar Prodigy, GE Medical, Madison, WI; software versions 8.8 and 11.4) using computer-generated and manually confirmed default lines on anterior view planogram. In our laboratory the coefficient of variation was 9.9% for fat mass measurements on the Lunar Prodigy (based on monthly values for water and methanol phantom assessments from January 2003 through December 2006). Reproducibility of DXA in children has been reported (26); however, because of concerns surrounding unnecessary radiation exposure in healthy children, scan reproducibility in children was not performed in our studies.

MRI

Whole-body MRI was performed to quantify (TAT) and subdepots SAT, VAT, and IMAT. A 1.5-T scanner was used (6X Horizon: GE, Milwaukee, WI) and images were created with T-weighted spin-echo sequence and a 210 ms repetition time and echo time of 17 ms. Subjects lay motionless on the scanner platform with arms extended above their heads. Transverse images were acquired for the whole body with a between-slice gap of 40 mm in taller pediatric subjects and 25 or 35 mm gaps for smaller pediatric subjects, generating between 30 and 40 image slices per subject. The SLICEOMATIC (TomoVision, Montreal, Canada) software was used to calculate cross-sectional tissue areas according to previously established protocols (27). AT volumes were

converted to mass using the estimated density of both tissues 0.92 kg/l (28). The interclass correlation coefficients among three analysts (who each read the same scans twice, separated by a 3-mo interval) for SAT, VAT, and IMAT in our laboratory are 0.99, 0.95, and 0.97, respectively.

Statistical Analysis

Descriptive statistics, mean and standard deviation, were calculated for continuous variables. For categorical variables, number and percentage were calculated for each level of the variable. The paired *t*-test was used to test the null hypothesis that the mean TAT was equal to the mean Fat_{DXA}. Multiple regression analysis was used to derive equations to predict TAT and each of the subdepots SAT, VAT, and IMAT using the T0 data. Potential independent variables for the regression equations included Fat_{DXA}, age, race, sex, Tanner stage, and their interactions. The backward-elimination method was used to select the subset of independent variables to retain in the prediction equations. The predicted residual sum of squares method (PRESS) was used to as an alternative to data splitting to validate the model (29). R^2_{PRESS} and the $\text{SEE}_{\text{PRESS}}$ statistics are provided to give an assessment of the validity of the equations. Although T1 and T2 follow-up data do not represent an independent data set, they were used to check the prediction equations. Descriptive statistics, mean, standard deviation, and interquartile range, were calculated for the difference between the predicted and measured values. The hypothesis that the mean difference was equal to zero was tested using a paired *t*-test. There were 22 children with follow-up data at T1 and T2. This sample size has a power of 80% to detect a difference of $0.6 \times (\text{SD of the difference})$ using a paired *t*-test (two-tailed) with a level of significance of 0.05. Separate analyses were performed for each variable.

All statistical analyses were performed using the SAS version 9.2 software package (SAS Institute, Cary, NC) for personal computer. The level of significance for all statistical tests of hypotheses was 0.05.

STATEMENT OF FINANCIAL SUPPORT

This work was supported by the National Institute of Child Health & Human Development (grant RO1 HD42187) and the National Institute of Diabetes & Digestive & Kidney Diseases (grants PO1 DK42618, P30 DK26687, and RR 024156).

REFERENCES

- de Onis M, Blössner M, Borghi E. Global prevalence and trends of overweight and obesity among preschool children. *Am J Clin Nutr* 2010;92:1257–64.
- Casazza K, Dulin-Keita A, Gower BA, Fernandez JR. Intraabdominal fat is related to metabolic risk factors in Hispanic Americans, African Americans and in girls. *Acta Paediatr* 2009;98:1965–71.
- Cruz ML, Bergman RN, Goran MI. Unique effect of visceral fat on insulin sensitivity in obese Hispanic children with a family history of type 2 diabetes. *Diabetes Care* 2002;25:1631–6.
- Taksali SE, Caprio S, Dziura J, et al. High visceral and low abdominal subcutaneous fat stores in the obese adolescent: a determinant of an adverse metabolic phenotype. *Diabetes* 2008;57:367–71.
- Lee S, Guerra N, Arslanian S. Skeletal muscle lipid content and insulin sensitivity in black versus white obese adolescents: is there a race differential? *J Clin Endocrinol Metab* 2010;95:2426–32.
- Ochiai H, Shirasawa T, Nishimura R, et al. Relationship of body mass index to percent body fat and waist circumference among schoolchildren in Japan—the influence of gender and obesity: a population-based cross-sectional study. *BMC Public Health* 2010;10:493.
- Baumgartner RN. Age. In: Heymsfield SB, Lohman TG, Wang Z, Going SB, eds. *Human Body Composition*. Champaign, IL: Human Kinetics, 2005:259–270.
- Knowles KM, Paiva LL, Sanchez SE, et al. Waist circumference, body mass index, and other measures of adiposity in predicting cardiovascular disease risk factors among Peruvian adults. *Int J Hypertens* 2011;2011:931402.
- Motala AA, Esterhuizen T, Pirie FJ, Omar MA. The prevalence of metabolic syndrome and determination of the optimal waist circumference cutoff points in a rural South african community. *Diabetes Care* 2011;34:1032–7.

10. Fujimoto WY, Bergstrom RW, Boyko EJ, et al. Visceral adiposity and incident coronary heart disease in Japanese-American men. The 10-year follow-up results of the Seattle Japanese-American Community Diabetes Study. *Diabetes Care* 1999;22:1808–12.
11. Brambilla P, Bedogni G, Moreno LA, et al. Crossvalidation of anthropometry against magnetic resonance imaging for the assessment of visceral and subcutaneous adipose tissue in children. *Int J Obes (Lond)* 2006;30:23–30.
12. Savva SC, Tornaritis M, Savva ME, et al. Waist circumference and waist-to-height ratio are better predictors of cardiovascular disease risk factors in children than body mass index. *Int J Obes Relat Metab Disord* 2000;24:1453–8.
13. Alzen G, Benz-Bohm G. Radiation protection in pediatric radiology. *Dtsch Arztebl Int* 2011;108:407–14.
14. Kim J, Shen W, Gallagher D, et al. Total-body skeletal muscle mass: estimation by dual-energy X-ray absorptiometry in children and adolescents. *Am J Clin Nutr* 2006;84:1014–20.
15. Dorsey KB, Thornton JC, Heymsfield SB, Gallagher D. Greater lean tissue and skeletal muscle mass are associated with higher bone mineral content in children. *Nutr Metab (Lond)* 2010;7:41.
16. Bridge P, Pocock NA, Nguyen T, et al. Validation of longitudinal DXA changes in body composition from pre- to mid-adolescence using MRI as reference. *J Clin Densitom* 2011;14:340–7.
17. Goran MI, Nagy TR, Treuth MS, et al. Visceral fat in white and African American prepubertal children. *Am J Clin Nutr* 1997;65:1703–8.
18. Bridge P, Pocock NA, Nguyen T, Munns C, Cowell CT, Thompson MW. Prediction of appendicular skeletal and fat mass in children: excellent concordance of dual-energy X-ray absorptiometry and magnetic resonance imaging. *J Pediatr Endocrinol Metab* 2009;22:795–804.
19. Rosenbaum M, Pietrobelli A, Vasselli JR, Heymsfield SB, Leibel RL. Sexual dimorphism in circulating leptin concentrations is not accounted for by differences in adipose tissue distribution. *Int J Obes Relat Metab Disord* 2001;25:1365–71.
20. Fuller NJ, Hardingham CR, Graves M, et al. Assessment of limb muscle and adipose tissue by dual-energy X-ray absorptiometry using magnetic resonance imaging for comparison. *Int J Obes Relat Metab Disord* 1999;23:1295–302.
21. Kullberg J, Brandberg J, Angelhed JE, et al. Whole-body adipose tissue analysis: comparison of MRI, CT and dual energy X-ray absorptiometry. *Br J Radiol* 2009;82:123–30.
22. Scherzer R, Shen W, Bacchetti P, et al.; Study of Fat Redistribution Metabolic Change in HIV Infection. Comparison of dual-energy X-ray absorptiometry and magnetic resonance imaging-measured adipose tissue depots in HIV-infected and control subjects. *Am J Clin Nutr* 2008;88:1088–96.
23. Fields DA, Goran MI. Body composition techniques and the four-compartment model in children. *J Appl Physiol* 2000;89:613–20.
24. Blake GM, Naeem M, Boutros M. Comparison of effective dose to children and adults from dual X-ray absorptiometry examinations. *Bone* 2006;38:935–42.
25. Park YW, Heymsfield SB, Gallagher D. Are dual-energy X-ray absorptiometry regional estimates associated with visceral adipose tissue mass? *Int J Obes Relat Metab Disord* 2002;26:978–83.
26. Figueroa-Colon R, Mayo MS, Treuth MS, Aldridge RA, Weinsier RL. Reproducibility of dual-energy X-ray absorptiometry measurements in prepubertal girls. *Obes Res* 1998;6:262–7.
27. Song MY, Ruts E, Kim J, Janumala I, Heymsfield S, Gallagher D. Sarcopenia and increased adipose tissue infiltration of muscle in elderly African American women. *Am J Clin Nutr* 2004;79:874–80.
28. Snyder WS, Cook MJ, Nasset ES, Karhansen, LR, Howells, GP, Tipton, IH. *Report of the Task Group on Reference Men*. Oxford, UK: Pergamon Press, 1975.
29. Holiday DB, Ballard JE, McKeown BC. PRESS-related statistics: regression tools for cross-validation and case diagnostics. *Med Sci Sports Exerc* 1995;27:612–20.